EXPERIMENTAL ANALYSIS OF THE EFFECT OF A WETTABILITY GRADIENT ON CONDENSATION HEAT TRANSFER COEFFICIENT

Mancio Reis F.M.[1,(α)], Lavieille P.[1] and Miscevic M.[1]*

[1]University of Toulouse, LAPLACE (Laboratory on Plasma and Conversion of Energy), Toulouse, France

((α)Mancio Reis F.M. is now at Altran SO.)

*Author for correspondence

University of Toulouse, LAPLACE (Laboratory on Plasma and Conversion of Energy),

UPS-INP-CNRS,

118 route de Narbonne,

31062 Toulouse Cedex 09, France

E-mail: marc.miscevic@laplace.univ-tlse.fr

NOMENCLATURE

h	$[W/m^2K]$	Heat transfer coefficient
T	$[K]$	Temperature
x	$[m]$	Cartesian axis direction
y	$[m]$	Cartesian axis direction

Special characters
φ	$[W/m^2]$	Heat flux

Subscripts
sat	Saturation
hfs	Heat flux sensor

ABSTRACT

The use of surfaces with wettability gradient aims to cover the surface with drops of small size to allow a large heat exchange. Thus, the action of the wettability gradient on the surface of the substrate is twofold: on the one hand, it allows the preservation of a dropwise condensation regime for which the heat exchange coefficient is particularly important and, on the other hand it allows the evacuation of the dispersed phase, thus promoting a renewal of the surface with very important heat exchanges during the nucleation phase. Thereby, a heat transfer enhancement factor up to 3.4 has been experimentally measured.

INTRODUCTION

When steam condenses on a wall, condensates may cover the surface in the form of a continuous liquid film, referred as filmwise condensation, or as a multitude of droplets, referred as dropwise condensation. If the surface is hydrophilic, nuclei spread out, coalesce, and a continuous film of condensate is formed. If the surface is hydrophobic, the condensates remain in the form of droplet clusters much longer. Dropwise condensation is preferable to filmwise condensation because the heat transfer coefficient can reach values one order of magnitude higher than those of the film condensation.

Two methods allow obtaining dropwise condensation regime.

The first consists in applying a permanent coating of a hydrophobic material on the wall. The second consists in adding to the steam a liquid or a gaseous product that is then adsorbed by the surface. For instance, Welch and Westwater [2] performed an experimental study of steam condensation on copper walls with and without the addition of copper oleate to the water used to generate the steam. They observed an important increase of the heat flux and of the heat transfer coefficient when the condensation occurs in the dropwise regime (with oleate of copper) compared to the case where the condensation occurs in the filmwise regime. Later, Takeyama and Shimizu [3] shown similar experimental results in the case of condensation of steam on vertical copper tubes : they observed higher heat transfer coefficients in the dropwise condensation regime than in the filmwise condensation regime. Nevertheless, the heat transfer coefficients in the two regimes tend towards the same values for the highest subcoolings. Thus, the dropwise condensation regime is extremely favourable when the saturation-to-wall temperature differences are weak.

In a previous study, a modelling of the growth and of the dynamic behaviour of a micro droplet placed on a wettability gradient surface was proposed [4; 5; 6]. Thanks to a wettability gradient printed on the surface of the substrate, it has been shown that it is possible to maintain the dropwise condensation regime in long duration experiments. The use of the wettability gradient on the surface allows covering the surface with drops of small size, resulting in an important heat transfer rate. Additionally, it allows the evacuation of the dispersed phase, thus promoting a renewal of the surface with very important heat exchanges during the nucleation phase.

Within this framework, the work presented in this paper focused on the quantification of the effect of the wall wettability heterogeneity on heat transfer from an experimental point of view. A particular application of this work concerns systems used in microgravity, for which it is crucial to understand and propose

an innovative and efficient technique allowing high heat transfer rates.

In the following, the chemical process allowing obtaining the wettability gradient surface is first described. Characterization and analysis of both contact angle and contact angle hysteresis (which are key parameters in the movement of a drop on any surface, see previous study [4; 5]) are then proposed. In a second step, the results obtained in condensation experiments with such a treated surface are presented.

CHEMICAL TREATMENT OF THE SUBSTRATE

In this section, the way used to create a wettability gradient with a relatively low contact angle hysteresis is described, as well as the results of the characterization of both the contact angle and the contact angle hysteresis.

The chemical treatment by silanization that we have implemented is inspired by the method used by Chaudhury and Whitesides [1]. The technique involves exposing a glass or silicon surface to the vapour diffusion front of a silane product. A drop of silane that evaporates leads to the formation of a concentration gradient in the gaseous phase in the vicinity of this drop. The closer the surface of the substrate is to the silane droplet, the greater the action of the silane. The contact angle on the surface is thus increased, i.e. the surface energy is decreased. The experimental device of the chemical treatment is shown in Fig. 1. It consists of a vacuum test chamber made of poly-methylmethacrylate (PMMA). The chemical process requires a dry environment, without any flow that could change the natural diffusion of the silane. The enclosure is thus perfectly sealed.
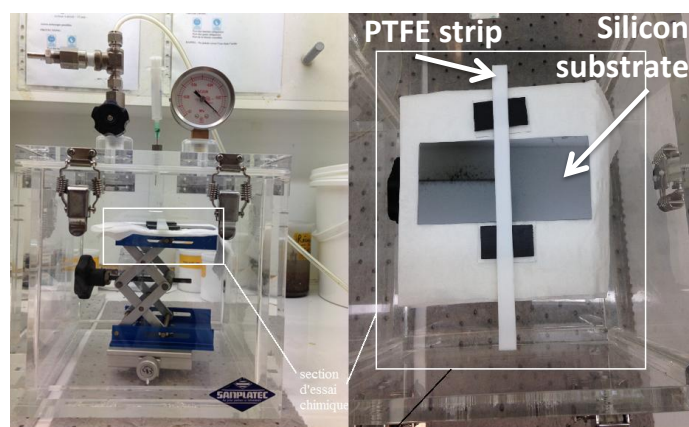

Figure 1. Apparatus developed to treat silicon or glass substrate. Left : side view. Right : top view; the substrate is here silicon, with the PTFE strip placed 2 *mm* above the substrate.

The clean substrate that has to be treated is placed on an elevating support. A drop of trichloro(octyl)silane is then placed on a strip of polytetrafluoroethylene (PTFE). Since PTFE is chemically inert, it is ensured that no chemical reaction pollutes the environment in the enclosure. This PTFE strip is positioned

so that the trichloro(octyl)silane drop is at the centre of the substrate at a distance of 1 to 2 mm above the substrate. The silane vapours then act on the sample for one minute and thirty seconds. The treated surface is then removed from the enclosure and immediately heated in an oven at 100°C during five minutes. This last step, referred to as annealing, allows the chemical bonds to be strengthened.

CHARACTERIZATION OF THE TREATED SURFACE

In a first step, we made measurements of contact angles on the whole of the sample using a Digidrop goniometer, by following a precise mesh. The red dots in fig. 2 represent the locations where the deposits of drops have been made and hence where the contact angles are known experimentally. The mesh is more refined at the centre, in the treated area, to obtain a more precise value of the gradient in this region. An interpolation function is used on the set of measured values using Matlab software. A complete mapping of the substrate is deduced by plotting the static angle as a function of the position as can be seen in fig. 2. The mapping allows us to see clearly the effect of the chemical treatment and to determine the zones where the gradient is the most important. The stronger the gradient, the more likely the droplet is to move. On the sample shown in fig. 2, the strongest value of the obtained gradient is about 10° per millimetre at approximately one centimetre from the centre.
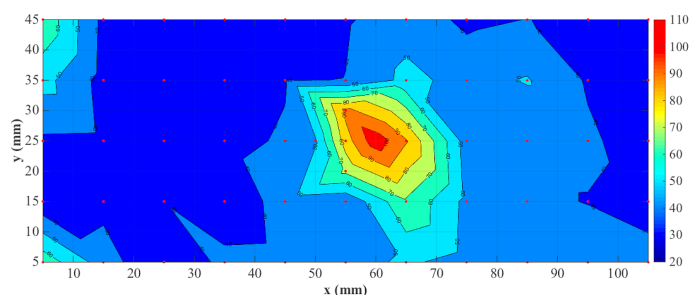

Figure 2. Mapping of the contact angles on a sample treated by silanization method. The red dots represent the points where the contact angle measurements were performed.

First, a drop is deposited on the substrate and the static contact angle is measured. To determine the contact angle hysteresis, we need to know both advancing and receding contact angles. In this aim, we first injected liquid in a droplet that has been deposited at a given position to determine the advancing contact angle; we then removed liquid from this droplet to determine the receding contact angle. Thus for each position we made videos of "inflation" and "deflation? of a droplet having a volume as smallest as possible (about 0.3 micro litre at deposition). An example of detection of dynamic contact angles is shown in fig. 3. When the drop inflates, the contact line only moves once the advancing contact angle has been reached. During the movement of the triple line, the advancing contact angle remains almost
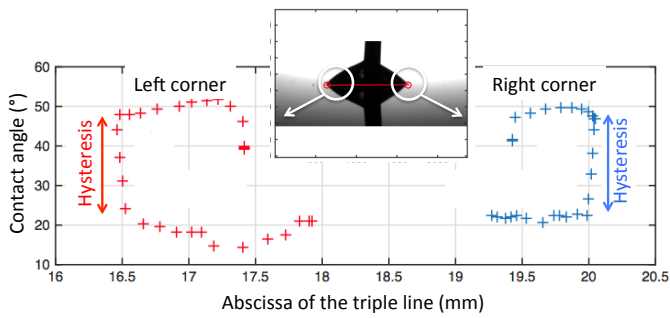
Figure 3. Example of hysteresis measurement at two given locations (left and right corners of the droplet) on the substrate.
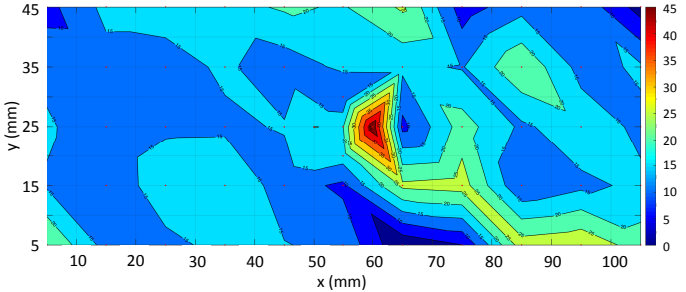

Figure 4. Mapping of the contact angle hysteresis on the same sample than in fig. 2 treated by silanization method. The red dots represent the points where the contact angle hysteresis measurements were performed.

constant. During the deflation phase, the contact line remains in the same position and the contact angle decreases down to the receding contact angle.

This graph shows that the value of the hysteresis is not the same on the right side as on the left side. This difference is caused by the gradient : the corner of the droplet that must climb the gradient will have more difficulty than the one that must descend it.

Then, values of the advancing and receding contact angles at each location of the sample are recorded and put into a spreadsheet to perform the mapping in the same way than previously. An example of the contact angle hysteresis field is reported in fig. 4. It can be seen from this figure that hysteresis of the contact angle is very heterogeneous. Indeed, we can observe important variations of the hysteresis on only a few millimetres. The highest values (up to $40 - 45°$) are obtained in the hydrophobic part, in the central area of the treated surface.

Profiles of the static and dynamic contact angles along the median axis of the sample are reported in fig. 5. Variations up to $90°$, $70°$ and $60°$ are obtained for the advancing, static and receding contact angles, respectively. For these three angles, the variations (increase and decrease) occur on a distance of approximately 25 mm, from $x = 55\ mm$ to $x = 80\ mm$.
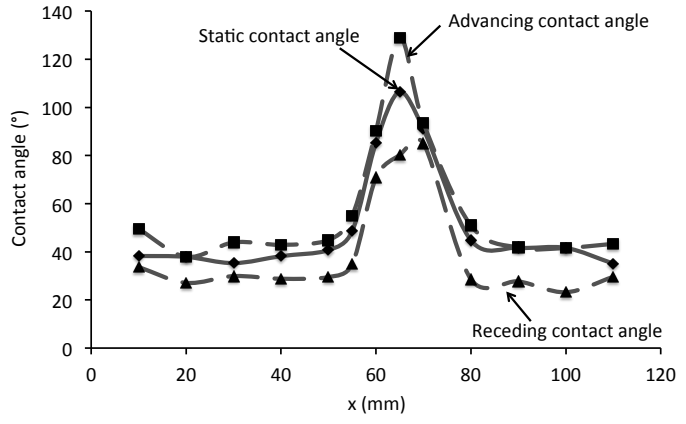

Figure 5. Axial variation of the static, advancing and receding contact angles along the median axis (y=25mm) for the same sample than fig. 2 and fig. 4

EXPERIMENTAL SETUP

The enclosure is a parallelepiped with rounded edges, of dimensions $200 \times 200 \times 160\ mm^3$ in duralumin (AU4G), with a thickness of $20\ mm$. To ensure that the inside of the enclosure remains visible, 4 Pyrex® windows are placed on the top, bottom and side faces. Each window is clamped between two fluorocarbon flat seals to ensure water tightness. A cylinder of $70\ mm$ in diameter, made also of duralumin, passes through the enclosure and serves as a support for the sample holder.
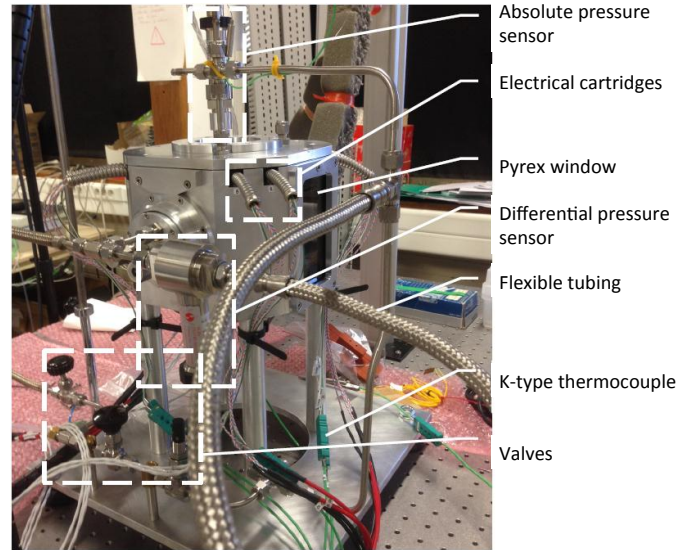

Figure 6. Photo of the experimental setup.

The sample holder is illustrated in fig. 7. The substrate is held on this holder by suction, thanks to a vacuum pump connected

to the cylinder. Simultaneously, the temperature (and thus the pressure) in the enclosure is imposed thanks to electrical cartridges inserted in the aluminum walls. A pressure difference between the enclosure and the inside of the cylinder is thus created. The advantage of this device is that the treated surface remains clean and devoid of any geometrical irregularity that could disrupt the flow of the drops on the surface. The sample holder is made of polyvinyl chloride (PVC) with a thermal conductivity $\lambda_{PVC} = 0.2 \ W.m^{-1}.K^{-1}$. It has the same surface area as the sample, i.e. $50 \times 110 \ mm^2$. During the condensation cycle, a water circuit connected to a temperature-controlled bath cools the plate. The exchanger in the centre of the sample holder has dimensions $10 \times 20 \times 26 \ mm^3$.
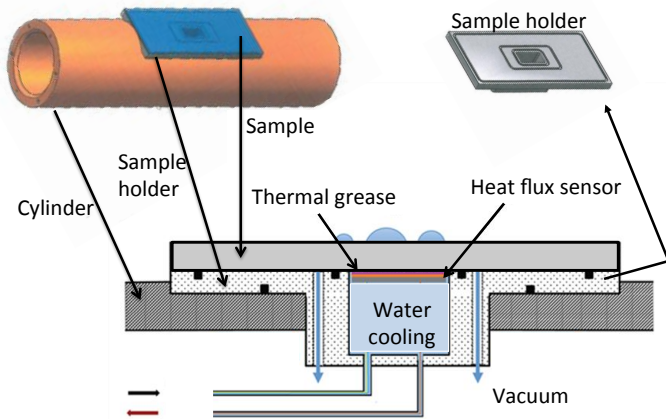

Figure 7. Schema of the sample holder showing the way used to ensure sealing and the cooling circuit.

The enclosure is connected to two pressure sensors: an absolute pressure sensor placed on the upper part in order to indicate the absolute pressure in the enclosure and a second sensor allowing measuring the pressure difference between the enclosure and the inside of the cylinder (fig. 6 and 7). The knowledge of this pressure difference is important in order to control the force that maintains the substrate on the sample holder. A heat flux sensor is glued on the bottom surface of the treated substrate. In order to ensure good contact between the bottom wall and the heat flux sensor, a thin layer of thermal paste (about several tens of μm, thermal conductivity $\approx 1 \ W.m^{-1}.K^{-1}$) is spread. A T-type thermocouple is integrated into the heat flux sensor.

RESULTS

Qualitative analysis

The aim of the study is to create a mechanical imbalance in the area of the droplet footprint in order to generate the movement of the droplet on the substrate in the case of systems where gravity can no longer be used as a mechanism for evacuating drops. This is why the experiments were carried out with horizontal samples.

The condensation experiments were carried out with a temperature of 70°C imposed in the enclosure. The cooling circuit is adjusted to provide a temperature of 5°C at the cryostat outlet. At the first instants of the video, the steam condensation occurs at the centre of the sample. The condensation regime is the dropwise regime on the hydrophobic part of the surface. As the intensity of the wettability gradient at the centre of the sample is weak (because of axisymmetry), the drops increase in volume and coalesce until reaching the high intensity gradient zone (fig. 8). They are then evacuated due to the Young's forces imbalance at the triple line.

The results showed that the existence of a wettability gradient allows maintaining dropwise condensation regime by evacuating toward the periphery all droplets reaching a certain critical radius. The mapping of the wettability gradient of fig. 2 shows that the gradient hardly reaches the degree per millimetre at the centre whereas at about one centimetre from the centre the slope is of the order of 10° per millimetre. It is therefore when the drops reach the maximum gradient zone, either by condensation or by coalescence between them, that they are set in motion by the Young-Dupré forces imbalance at the triple line. It is found that after a few hours, a film of about 3 mm thickness covers the entire untreated area. On the treated area, the surface is permanently renewed; the condensation regime in drops is preserved despite the surface being horizontal.

Instantaneous heat transfer coefficient evolution

As the heat flux (φ) and the temperature within the heat flux sensor (T_{hfs}) and in the enclosure (T_{sat}) are measured, a heat transfer coefficient can be deduced:

$$h = \frac{\varphi}{T_{sat} - T_{hfs}}$$

It should be noticed that this heat transfer coefficient is not the heat transfer coefficient between the fluid and the substrate's wall, as it includes the contact thermal conductance between the substrate and the heat flux sensor. The real condensation heat transfer coefficient is thus a little bit higher than the one reported in the following.

The evolution of this heat transfer coefficient as a function of time is reported in fig. 9. During the first 50 seconds, it can be observed that the coefficient reaches high values (up to $7700 \ W.m^{-2}.K^{-1}$ at approximately 20 seconds) and then drops rapidly down to a value of the order of $200 - 300 \ W.m^{-2}.K^{-1}$. During this transient phase, the peak of the very first moments is due to the appearance of the micro droplets that, because of their micrometrical dimension greatly favour the heat exchanges.

The droplets quickly reach a millimetre size, which causes the heat exchange coefficient to drop. Between 10 and 50 minutes the heat transfer coefficient increases, although the drops continue to increase. During this period, the condensation regime is the dropwise regime over the entire substrate surface (including the untreated zone). The displacements of the drops are observed
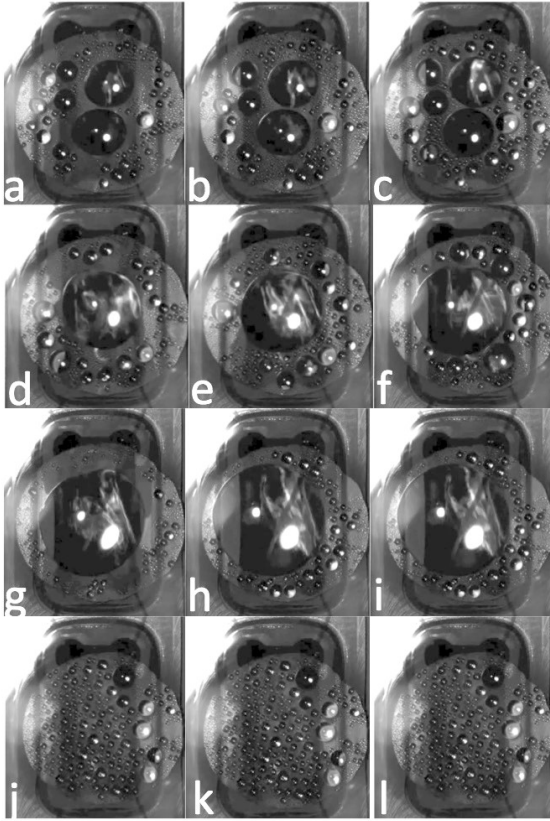
Figure 8. Top view of the condensation process. Droplets nucleate, grow, coalesce up to a certain radius. The biggest droplets are evacuated to the periphery of the treated zone and new nuclei appear. The duration between photo (a) and photo (l) is about 4 seconds.

within the circular chemically treated zone, at the centre of the substrate (circular surface of diameter approximately 3 cm). The fact that the condensation regime is dropwise regime on the whole plate and that the large drops in the centre are evacuated allows the heat transfers to be improved. Moreover, the evacuation of the drops creates dry zones that are very interesting from a thermal point of view: these zones are freed to generate micro drops, which promote the heat exchanges. The heat transfer coefficient is thus increased by about 40% (from 275 $W.m^{-2}.K^{-1}$ to 380 $W.m^{-2}.K^{-1}$) during about forty minutes. Finally, after one hour of condensation on the surface, the liquid film becomes clearly visible outer of the treated zone. The longer the time elapses, the thicker and wider it becomes, while the permanent evacuation of the condensates is maintained thanks to the wettability gradient. The film thickens, which increases the thermal resistance, while in the centre region the large drops are evacuated. Finally, an equilibrium is created between the two, thus stabilizing the curve around an average value of 375 $W.m^{-2}.K^{-1}$. After a condensation cycle the plate loses its wettability gradient capacities. Indeed, it ages and the characterization with Digidrop shows that the contact angles in the hydrophilic part substantially increase. On the other hand, the treated zone remains nearly un-
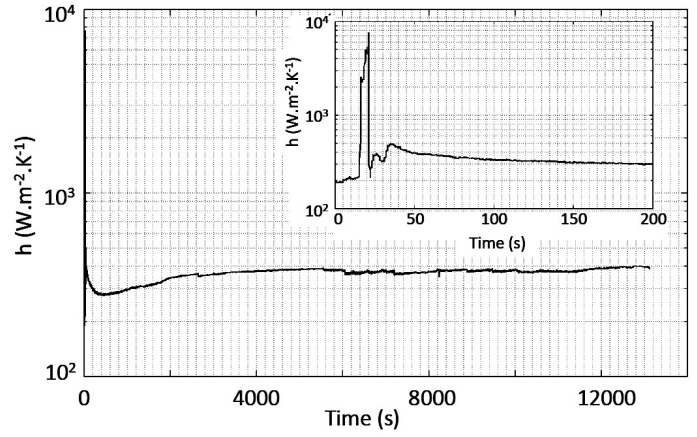

Figure 9. Heat transfer coefficient versus time. The insert is a zoom of the evolution of the heat transfer transfer coefficient in the 200 first seconds.
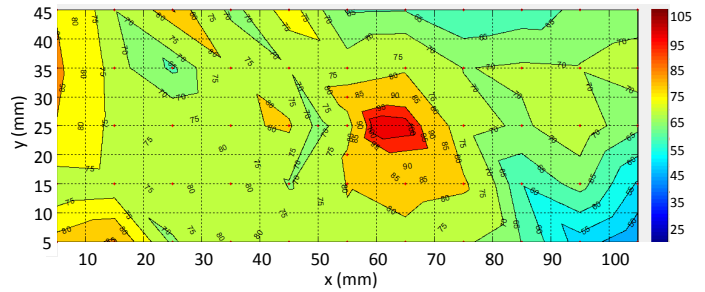
changed (fig. 10).

Figure 10. Mapping of the static contact angle on the sample treated by silanization method after a condensation cycle. An increase of the contact angle in the hydrophilic region is observed while hydrophobic part remains unchanged.
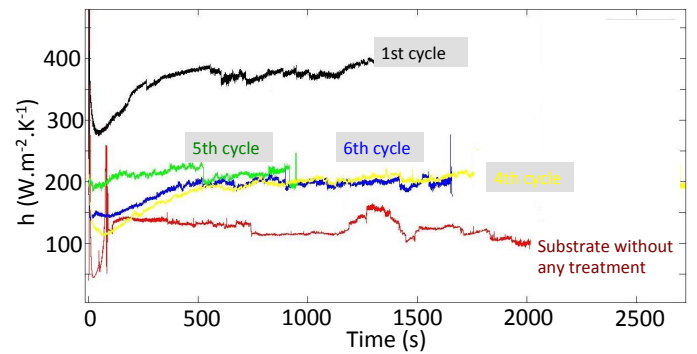

Figure 11. Variation of the heat transfer coefficient as a function of time for successive condensation cycles: from the 4th cycle the substrate has reached a final stage of aging (2nd and 3rd condensation cycles data have not been recorded).

150

We then made some experiments to assess if the plate ages asymptotically, or in other words if the sample no longer ages after a certain number of condensation cycles. For this we have made additional condensation cycles on the sample considered in fig. 9. The sample has undergone in total six cycles of condensation, the first being the one previously presented. The results are shown in fig. 11 for cycles 1, 4, 5 and 6. These curves are compared to a condensation cycle on a reference sample for which no surface treatment has been done (silicon in the raw state).

The results show that after the end of the 4th cycle, the silicon sample has reached a final stage of aging. For cycles 4, 5 and 6, almost a same value of the heat transfer coefficient is obtained, approximately equal to 200 $W.m^{-2}.K^{-1}$. Thermal exchanges are then half the ones of the first cycle. Nevertheless, all the heat transfer coefficients obtained with the treated surface remain above the heat transfer coefficient obtained with the reference sample. In this latter situation, the heat transfer coefficient in the pseudo-permanent regime, is about 110 $W.m^{-2}.K^{-1}$. The wettability gradient thus allows to almost double the heat transfer performances on the sample having undergone an aging. If one considers the performances on a substrate undergoing the first cycle of condensation (therefore with a strong gradient), the enhancement ratio is 3.4 with respect to the test sample.

CONCLUSION

An experimental bench was developed for the purpose of understanding and analysing the effects of surface energy gradients on heat transfers with condensation phase change. The realization of surfaces with a wettability gradient makes it possible to obtain drops of very small size, favouring the heat transfers. The results showed that the existence of such a gradient allows maintaining a dropwise condensation regime, even in the case of systems where gravity can no longer be used as a mechanism for evacuating drops. The analysis of the results also showed that the wettability gradient surface leads to an heat transfer enhancement: the heat transfer coefficient has been found to be roughly 3.4 times greater than the one measured on an untreated surface in the pseudo-permanent regime.

ACKNOWLEDGMENT

REFERENCES

[1] Chaudhury M.K. , and Whitesides G.M. , How to make water run uphill, *Science*, Vol. 256(5063), 1992, pp. 1539-1541.

[2] Welch J.F. , and Westwater J.W., Microscopic study of dropwise condensation, *International Developments in Heat Transfer*, Vol. 2, 1961, p. 302.

[3] Takeyama T., and Shimizu S, On the transition of dropwise condensation, *Proceedings of the 5th International Heat Transfer Conference*, Vol. 3, 1974, p. 274.

[4] Mancio Reis F.M., Lavieille P., and Miscevic M., Toward enhancement of water vapour condensation using wettability gradient surface, *Experimental Thermal and Fluid Science*, Vol. 67, 2015, pp. 70-74.

[5] Mancio Reis F.M., Lavieille P., Blanco S., and Miscevic M., On the effect of the contact angle hysteresis for small droplets on a wettability gradient surface, *Interfacial Phenomena and Heat Transfer*, Vol. 4, No 1, 2016, pp. 81-91.

[6] Mancio Reis F.M., Lavieille P., and Miscevic M., Dropwise condensation enhancement using a wettability gradient, *Heat transfer Engineering*, Vol. 38, No 3, 2017, pp. 377-385.